Journal of Thermal Analysis and Calorimetry, Vol. 88 (2007) 3, 769–774

STUDY OF THE COMPOSITION AND GAS-PHASE RELEASE CHARACTERISTICS OF SALT MATERIAL EXTRACTED FROM MSW ASH PARTICLES USING STA

S. Arvelakis[1*], *F. J. Frandsen*[1] *and E. G. Koukios*[2]

[1]CHEC Research Group, Department of Chemical Engineering, Technical University of Denmark, (DTU), Lyngby 2800, Denmark
[2]Bioresource Technology Unit, Department of Chemical Engineering, National Technical University of Athens
Zografou Campus, 15700 Athens, Greece

The ash material generated from the MSW incineration contains large amounts of alkali metals, heavy metals, chlorine and sulfur mainly deposited as inorganic salts and/or oxides on the surface of the Si-rich ash particles. In this work, the composition and gas-phase release characteristics of salt material extracted from MSW ash particles using a six-stage leaching process is studied using simultaneous thermal analysis (STA). The produced results provide useful information regarding the composition of the salt material and its melting behavior that is considered to play an important role to deposition and corrosion problems at MSW incinerators. The results may be used to model the deposition process and to the better understanding of the corrosion process during MSW incineration.

Keywords: *ash, corrosion, deposition, MSW, salts, STA*

Introduction

The growing demand of energy today in combination with the high prices of oil fuel and increased concern of the use of coal for power generation due to the high emissions of CO_2 that accelerates the greenhouse effect has lead to the need for exploitation of new and renewable energy sources. At the same time the increased production of municipal solid waste (MSW) material in the developed world and the environmental concerns, their safe and economical disposal brings with, has lead to the consideration of MSW material not as a waste stream but rather as an attractive 'green' solid fuel. Incineration of MSW is becoming a more attractive alternative than the traditional means of disposal via landfilling because this method is technically proven as an effective, economical and environmentally safe waste treatment technology [1, 2]. According to the new EU legislation directive 1999/31/EU the amount of waste material for landfilling should be limited to the 75 mass/mass% of the quantity landfilled in 1995 by 2010. Furthermore, no waste material containing more than 5% biodegradable carbon will be allowed to landfill [3]. However, though the new MSW incineration plants equipped with modern pollution control devices have met the environmental problems such as dioxins emissions, odour, noise, etc. successfully there are still problems that have to be solved to improve mainly the economics and the efficiency of the process [4–10]. These problems are mainly associated with the ash generated during the MSW incineration. The produced ash material is rich in alkali metals, chlorine, sulfur as well as heavy metals like Zn, Pb, Ni, Cd, etc. These inorganic compounds included in the original MSW material tend to react during the incineration process and to form gases, liquids and solids that cause severe ash-related problems such as deposition and corrosion. The need to mitigate these problems leads to lower steam temperatures, use of more expensive steel alloys for heat exchangers as well as to unscheduled shut-downs for cleaning and repairing the corroded surfaces. This leads to higher operational costs, lower availability and lower efficiency compared to the coal-fired plants. Furthermore, the produced ash material needs to be treated and stabilized before further use due to the high amounts of heavy metals into reactive forms such as chlorides $ZnCl_2$, sulfates $PbSO_4$, $ZnSO_4$ and oxides ZnO, PbO, etc. [6, 11–14].

The determination of the melting and gas phase release behavior of the salt material deposited on the surfaces of the ash particles during the MSW incineration process could be of premium importance, to assist with the mitigation of the ash-related problems and the ash disposal. In the present study thermal analysis was applied to characterize the salt material extracted from various MSW ash fractions. Thermal analysis is widely used in combustion research for the determination and understanding of various properties and the behavior of different fuels under a wide range of conditions and applications [15–17]. It has

* Author for correspondence: sarvel_1999@yahoo.com

1388–6150/$20.00

Akadémiai Kiadó, Budapest, Hungary
Springer, Dordrecht, The Netherlands

been reported that thermal analysis methods including TG/DTA, TG/DSC, TMA and DMA can be used to provide an estimation regarding the ash melting characteristics of various coal, waste and biomass samples [18–20]. In this work a TG/DSC Instrument (thermogravimetric analysis/differential scanning calorimetry) also called an STA (simultaneous thermal analysis) instrument is used to characterize the melting and gas-phase release characteristics of the salt material extracted from the surface of four MSW ash fractions using a six-stage leaching process.

In this paper the melting behaviour and gas-phase release characteristics of four different ash fractions generated from the incineration of MSW material is studied using simultaneous (DSC/TG) thermal analysis.

Experimental

Materials and methods

The material used in this study is different ash fractions from the Horsens MSW incinerator in Denmark. Four different ash fractions, from two different boilers, 2–3rd pass ash, super-heater ash, economizer ash and ash from the electrostatic precipitator, were collected. All the initial ash samples were leached using a six-stage leaching process to remove the water-soluble salts condensed on the surface of the ash particles, in order to study their melting behavior as well as their gas-phase release characteristics [21]. A part of the salt material extracted after each leaching stage was kept dried in an evaporation oven at 110°C and was kept for the STA tests. The remaining liquid samples were mixed homogenized and after evaporation in the furnace the recovered salt material constituted the total salt material removed from each ash fraction during the leaching process. The total salt fractions were used for the STA tests.

A Netzsch STA 409 C was used in the present investigation. A detailed description of the STA process can be found elsewere [22].

The specific STA measurements included the following steps:

5–10 mg of the salt sample, is placed in a 30 mL platinum/rhodium crucible. Between the platinum crucible and the platinum sample carrier a disc of aluminum is placed, to prevent the two parts sticking to each other during experiments. Lids cover the crucible in order to obtain a more uniform temperature distribution inside. A hole in the lids allows the escape of evaporation products. A second crucible (the reference) contains about 19–20 mg of α-Al_2O_3. A flow rate of pure nitrogen of 100 mL min^{-1} keeps inert conditions in the oven and removes any gaseous products released. The sample is heated at a heating rate of 10°C min^{-1} to 1500°C where the experiment ends. The temperatures of the sample and reference are recorded by a Pt–Rh thermocouple (type S) and a high precision balance registers potential mass loss due to evaporation/decomposition of the sample. After the end of each STA test the sample crucible was visually inspected in order to define the final condition of the sample material and to correlate it with the results derived from the generated STA curves.

Results and discussion

Table 1 presents the elemental analysis of the different ash fractions sampled from different sections of two boilers at Horsens MSW plant, before and after the leaching process. The elemental analysis was performed using the inductively coupled plasma-optical emission spectroscopy (ICP-OES) method. Ash fractions are seen to contain more alkali metals, in the order economizer<2–3rd pass<super-heater<ESP, chlorine in the order 2–3rd pass<economizer< super-heater<ESP, sulfur in the order economizer< super-heater<ESP<2–3rd pass and zinc in the order economizer<super-heater<2–3rd pass<ESP. The ashes from both boilers show to have similar compositions, while some variation is also observed. In general, the ash fractions from the boiler 1 are seen to have lower concentrations of alkali metals and higher in chlorine and sulfur compared to the fractions from boiler 2. The leaching process is seen to remove alkali metals and chlorine in the order economizer<super-heater< 2–3rd pass<ESP and sulfur in the order economizer< 2–3rd pass<super-heater, while the amount of sulfur in the ESP fraction is seen to increase after the leaching process, from the surface of the ash particles. These results show that sulfur is deposited in the ash particles in mainly water-soluble forms in the sections of the boiler where higher temperatures prevail, while chlorine and alkali metals follow the same removal pattern. Aluminum, silica, calcium, magnesium, as well as zinc and the other elements are seen to increase in concentration as they are present in non water-soluble forms [21].

Table 2 presents the mass/mass% of water-soluble salt material contained in every ash fraction. As it is seen from Table 2 the ESP ash fractions contain the highest amounts of water-soluble salt material compared to the other ash fractions. The 2–3rd pass and economizer ash fractions from boiler 2 are seen to contain higher amounts of water-soluble salts compared to the fractions from boiler 1. On the contrary, ESP and super-heater ash fractions from boiler 1 contain higher amounts compared to the fractions from boiler 2. However, all the ash fractions are seen to

Table 1 Chemical composition of the ash samples using ICP-OES (mass/mass%)

Sample	Al_2O_3	SiO_2	K_2O	Na_2O	CaO	MgO	Fe_2O_3	P_2O_5	SO_3	TiO_2	ZnO	Cl
2–3rd pass ash non-leached 1	9.82	19.71	3.86	3.91	25.20	3.00	2.71	3.21	19.00	2.00	1.74	2.10
2–3rd pass ash leached 1	10.58	23.14	0.94	1.32	28.56	3.67	3.29	3.66	15.25	2.50	1.87	0.04
Difference/%	7.69	17.39	– 75.63	– 66.21	13.33	22.22	21.05	14.29	– 19.74	25.00	7.14	– 98.33
2–3rd pass ash non-leached 2	10.20	21.64	4.10	4.18	24.92	3.00	2.43	3.21	16.75	2.00	1.62	1.80
2–3rd pass ash leached 2	11.90	24.43	1.21	1.48	27.72	3.50	3.14	3.62	12.75	2.33	1.74	0.05
Difference/%	16.67	12.87	– 70.59	– 64.52	11.24	16.67	29.41	12.86	– 23.88	16.67	7.69	– 97.22
S-heater ash non-leached 1	11.52	22.71	4.22	4.31	23.66	2.67	4.00	4.58	11.00	2.17	0.88	2.90
S-heater ash leached 1	12.84	27.43	1.33	1.75	26.88	3.17	4.43	5.50	8.00	2.83	1.02	0.11
Difference/%	11.48	20.75	– 68.57	– 59.38	13.61	18.75	10.71	20.00	– 27.27	30.77	15.49	– 96.21
S-heater ash non-leached 2	10.58	22.71	3.86	3.91	23.80	2.67	4.57	4.58	10.25	2.17	0.77	3.10
S-heater ash leached 2	11.90	26.79	1.33	1.75	26.74	3.17	4.57	5.50	8.25	2.50	0.93	0.11
Difference/%	12.50	17.92	– 65.63	– 55.17	12.35	18.75	0.00	20.00	– 19.51	15.38	20.97	– 96.45
Economizer ash non-leached 1	11.14	23.79	3.25	3.50	23.94	2.67	3.86	4.58	7.50	2.33	0.69	2.70
Economizer ash leached 1	13.22	28.93	1.45	2.02	26.32	3.17	4.14	5.50	6.50	2.67	0.82	0.12
Difference/%	18.64	21.62	– 55.56	– 42.31	9.94	18.75	7.41	20.00	– 13.33	14.29	20.00	– 95.56
Economizer ash non-leached 2	11.33	24.43	3.49	3.64	23.66	2.67	3.86	4.58	8.25	2.17	0.70	2.70
Economizer ash leached 2	13.22	27.64	1.45	1.89	25.90	3.00	4.57	5.50	7.00	2.67	0.86	0.11
Difference/%	16.67	13.16	– 58.62	– 48.15	9.47	12.50	18.52	20.00	– 15.15	23.08	23.21	– 95.93
ESP ash non-leached 1	3.97	7.29	4.46	3.91	32.48	1.52	1.43	1.42	10.25	0.77	3.36	23.00
ESP ash leached 1	8.12	15.43	0.64	0.85	36.26	3.00	3.29	2.75	17.75	1.55	6.48	0.19
Difference/%	104.76	111.76	– 85.68	– 78.28	11.64	97.80	130.00	93.55	– 73.17	102.17	92.59	– 99.17
ESP ash non-leached 2	5.48	10.29	4.58	4.04	32.20	1.83	2.14	1.92	10.25	0.93	2.74	18.60
ESP ash leached 2	9.07	17.57	0.60	0.84	37.10	3.00	3.86	3.02	14.50	1.60	4.36	0.17
Difference/%	65.52	70.83	– 86.84	– 79.33	15.22	63.64	80.00	57.14	– 41.46	71.43	59.09	– 99.09

Table 2 Water-soluble salt material contained in every ash fraction/mass%

Sample	Water-soluble salts/mass%
2–3rd pass ash non-leached 1	11.55
2–3rd pass ash non-leached 2	12.84
S-heater ash non-leached 1	12.6
S-heater ash non-leached 2	11.65
Economizer ash non-leached 1	8.92
Economizer ash non-leached 2	10.5
ESP ash non-leached 1	39.61
ESP ash non-leached 2	31.6

contain comparable salt amounts apart from the ESP fractions where the difference is seen to reach 25 mass/mass%.

The differences are attributed to variations in the MSW feeding stream to the boilers as well as to differences in the operating conditions of the two MSW boilers such as temperature, residence time as well as the boiler geometry.

2–3rd pass salts

Figure 1 and Table 3 present the results from the STA runs performed using the salt material extracted from the 2–3rd pass ash fractions during the six-stage leaching process. Both STA curves are seen to be similar till the 600°C and they show one endothermic peak at 514°C corresponding to the melting of the salt material. The very low melting temperature of the salt material is attributed to the interaction of the different salt compounds that tend to form binaries, ternaries, etc., mixtures that have melting points significantly lower compared to the pure compounds [22]. After the 600°C the curves are seen to be somewhat different. The salt sample from boiler 2 shows an endotherm starting at 654°C with peaks at 843 and 904°C that ends at 1050°C. A second endotherm starts at 1112°C with peaks at 1301 and 1397°C ending at 1428°C. The endotherms are accompanied by a mass loss that according to Table 3 is almost 5 mass/mass% in the segment 300–850°C due to the decomposition of calcium carbonate, while a mass loss of 21.61 mass/mass% is seen in the segment 850–1150°C mainly due to the evaporation of KCl, NaCl and to some extent to the decomposition of K_2CO_3, Na_2CO_3 and the release of CO_2 [22, 23]. Finally, a mass loss of 40 mass/mass% is observed in the temperature segment 1150–1450°C. At this temperature segment the decomposition of carbonates is concluded and the remaining CO_2 as weel as all the K_2O, Na_2O are evaporated. Furthermore, calcium and potassium/sodium sulphates as well as sulfides are partially decompose/evaporate increasing the observed mass loss. On the contrary, the salt sample

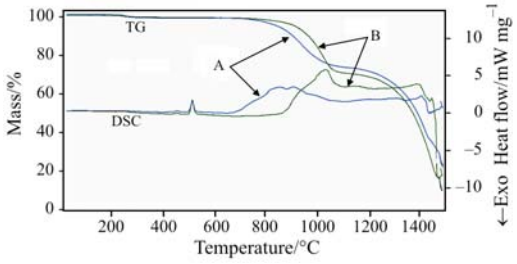

Fig. 1 Simultaneous thermal analysis of the 2–3rd pass salt samples; A – salt sample from boiler 1, B – salt sample from boiler 2

Table 3 Results from the STA runs using the extracted salt material from various ash fractions from MSW incineration

Salt sample	Mass loss during various temperature segments/mass%		
	300–850°C	850–1150°C	1150–1450°C
2–3rd pass salt boiler 1	2.32	27.4	50.65
2–3rd pass salt boiler 2	4.97	21.61	40.12
S-heater salt boiler 1	4.54	43.81	37.03
S-heater salt boiler 2	9.94	44.87	29.56
Economizer salt boiler 1	11.25	44.6	28.87
Economizer salt boiler 2	11.29	40.9	31.09
ESP salt boiler 1	0.88	40.64	38.87
ESP salt boiler 2	1.33	53.14	28.34

from boiler 1 is seen to have a lower mass loss (50 mass/mass%) in the segment 300–850°C and higher mass losses of 27.4 and 50.65 mass/mass% in the next two segments. A large endotherm is now seen to start at 850°C with a peak at 1027°C and ending at 1093°C. A second endotherm is seen at higher temperatures starting at 1242°C and ending at 1450°C giving two peaks at 1385 and 1437°C. The produced results agree with the results from Table 2 that shows that the salts from boiler 1 contain more chlorine and sulfur and as a result are expected to experience higher mass losses at high temperatures.

Super-heater salts

Figure 2 presents the results from the STA tests with the salt samples produced after the extraction of the super-heater ash fractions. The two STA curves are seen to be similar again till the temperature of 600°C. A melting endotherm is seen to appear at 517°C in both cases. In the case of the salt sample from boiler 1

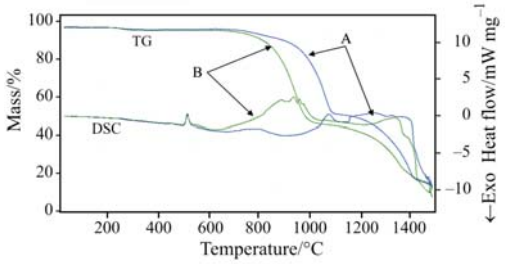

Fig. 2 Simultaneous thermal analysis of the super-heater salt samples; A – salt sample from boiler 1, B – salt sample from boiler 2

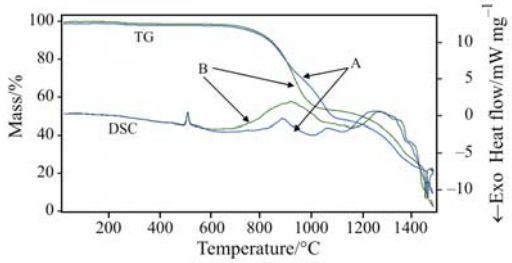

Fig. 3 Simultaneous thermal analysis of the economizer salt samples; A – salt sample from boiler 1, B – salt sample from boiler 2

a large endotherm is seen to start at 680 and ends at 879°C. A mass loss of 4.54 mass/mass% due to $CaCO_3$ decomposition is observed. A second endothermic reaction is seen to start at 949 and finishing at 1121°C. This is followed by a third endotherm starting at 1152 and ending at 1405°C. A mass loss of 43.81 mass/mass% is seen at the temperature segment 850–1150°C and a loss of 37.03 mass/mass% in the segment 1150–1450°C. The salt sample from boiler 2 shows a big endotherm starting at 638 and ending at 1028°C accompanied by total mass loss of 54.81 mass/mass% in the segment 300–1150°C. A final endotherm starts at 1240 and ends at 1428°C accompanied by a mass loss of 29.56 mass/mass%. Comparison of the results from the two STA curves shows that the salt sample from boiler 1 contains less $CaCO_3$, equal amounts of alkali chlorides and slightly higher amounts of alkali carbonates and sulfates compared to the salt sample from boiler 2.

Economizer salts

Figure 3 presents the results from the salt samples produced from the leaching of the economizer ash fractions. As it is seen from Fig. 3 the STA curves show a better match now compared to the former salt samples. The melting of the salt samples is seen to take place at 514°C. The salt from boiler 1 is seen to create three endothems above 600°C with the first starting at 710 and ending at 997°C. The second starting at 1013 and ending at 1124°C, and the third starting at 1124 and ending at 1447°C. The salt from boiler 1 is seen to create two large endotherms above 600°C. The first starts at 692°C with a peak at 918°C and ends at 1051°C, while the second starts at 1153 and ends at 1410°C showing a peak at 1277°C. Table 3 shows that the mass loss observed into the different temperature segments are also similar now. This is in good agreement with the results from Table 2 that show that the salt material extracted from both ash fractions have very similar composition regarding alkali metals, calcium, sulfur and chlorine. The observed mass loss is seen to be higher compared to the salt samples from the 2–3rd pass and the super-heater sections in the first temperature segment and from the 2–3rd pass samples in the second temperature segment, while they are at the same range compared to the super-heater salt samples in the second and third temperature segment and considerably lower compared to the 2–3rd pass samples in the third temperature segment.

ESP salts

Figure 4 presents the results from the STA measurements with the ESP salt samples. Both STA curves show a small endotherm around 140–150°C accompanied by a mass loss of 9–11 mass/mass% due to moisture evaporation. Both STA curves are seen to have a very good match compared to the previous salt samples. The melting of the salt samples is seen to take place for the salt from boiler 1 at 510°C and from boiler 2 at 530°C. Both salt samples show a large endotherm starting above 900°C creating peaks at various temperatures and ending at 1402°C for the salt from boiler 1 and at 1360°C for boiler 2.

Both salt samples show a very small mass loss below 850°C (1 mass/mass%). The salt sample from boiler 1 shows a smaller mass loss in the temperature segment 850–1150°C and a higher in the segment 1150–1450°C compared to the salt sample from boiler 2. Table 2 shows that the salt from boiler 1 contains lower amounts of alkali metals compared to the salt from boiler 2. The chlorine extracted from the ESP fraction from boiler 1 is seen to be significantly higher compared to that from the ESP fraction from boiler 2. However, the alkali concentrations show that the majority of this chlorine content is present probably as HCl which is removed from the leachate during its evaporation process. The higher mass loss observed at higher temperatures for the salt from boiler 1 shows that this sample contains higher amounts of alkali carbonates and sulfates compared to the salt from boiler 2. Comparison of the STA results with the results from the previous salt fractions shows that the ESP salts show similar mass loss in the segments 850–1150 and 1150–1450°C compared to the salts from the economizer and the super-heater areas. Exceptions is seen in the case of the ESP salt from boiler 2 that shows

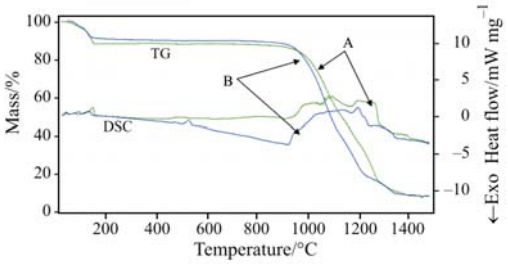

Fig. 4 Simultaneous thermal analysis of the ESP salt samples; A – salt sample from boiler 1, B – salt sample from boiler 2

significantly higher mass loss in the segment 1150–1450°C as well as the ESP salt and the super-heater salt from the boiler 1 in the segment 1150–1450°C.

Conclusions

Simultaneous thermal analysis provides valuable information regarding the thermal behaviour of the various salt fractions studied. The higher mass loss at high temperatures is observed mainly in the cases of the salt samples resulted from the cooler areas of both boilers such as the ESP and the economizer samples. The total mass loss in the segment 300–1450°C is seen to be similar for all the different salt samples with the exception of the 2–3rd salt from boiler 2. The results from the STA measurements are in good agreement with the results from the elemental analysis of the ash fractions before and after the leaching process. The mass loss observed during the STA tests assists in interpreting the composition of the salt samples from the different boiler sections.

The salts are seen to contain mainly alkali chlorides and carbonates as well as alkali and calcium sulfates. Since calcium sulphates are basically insoluble to water the results are evidence that the salts create binary, and/or ternary, etc. systems that are partially water-soluble. The mass loss curves as well as the DSC data show evidence that the multicomponent systems of insoluble/water-soluble salts melt at lower temperatures and show higher evaporation tendencies. This is evidence that the specific systems are more reactive now and may also play a more significant role in the formation of the ash deposits as well as in the corrosion process in the MSW boilers. The composition is seen to vary between the two boilers which indicates that the boilers are not operating under the same conditions as well as variations in the feeding streams.

All the STA curves are seen to match in the first heating stage up to 600°C presenting their melting peak in the same temperature area 510–530°C. At higher temperatures the STA curves from the ESP and the economizer salts show to have the best match.

The mass loss is seen to be mainly due to the dissociation of $CaCO_3$ below 850°C, the melting and evaporation of alkali chlorides as well as the partial dissociation of alkali carbonates below 1150°C and to the dissociation of alkali carbonates as well as alkali and calcium sulfates above 1150°C.

The STA results from the salt fractions may be used in combination with the ash elemental analyses to control the deposition and corrosion problems during the incineration process. Furthermore, as input data for the development of models for the prediction of the corrosion and deposition problems, during MSW incineration.

References

1 X. Guo, Z. Wang, H. Li, H. Huang, C. Wu and Y. Chen, Energy Fuels, 15 (2001) 1441.
2 C. Dong, B. Jin, Z. Zhong and J. Lan, Energy Convers. Manage., 43 (2002) 2189.
3 Directive 1999/31/EU, www.europa.int.
4 S. V. Vassiliev, C. Danheux, Ph. Laurent, T. Thiemann and A. Fontana, Fuel, 78 (1999) 1131.
5 CRC Handbook of Chemistry and Physics, 77th Ed., 1996–1997.
6 C. C. Wiles, J. Hazardous Mater., 47 (1996) 325.
7 A. Porteous, Appl. Energy, 70 (2001) 157.
8 E. Desroches-Ducarne, E. Marty, G. Martin and L. Delfosse, Fuel, 77 (1998) 1311.
9 L. Ruth, Prog. Energy Combust. Sci., 24 (1998) 545.
10 C. Dong, B. Jin, Z. Zhong and J. Lan, Energy Convers. Manage., 43 (2002) 2189.
11 T. R. P. E. Miles, T. R. Miles Jr., L. L. Baxter, R. W. Bryers, B. M. Jenkins and L. L. Oden, Alkali Deposits Found in Biomass Power Plants, Vol. I, II, NREL Subcontract TZ-2- 11226-1, 1995.
12 M. Spiegel, Molten Salt Forum, 7 (2003) 253.
13 M. Spiegel, Mater. Sci. Forum, (2001) 971.
14 H. H. Krause, Proceedings of the International Conference on Fireside Problems While Incinerating Municipal and Industrial Waste, 1989.
15 M. V. Kök, J. Therm. Anal. Cal., 68 (2002) 1061.
16 M. Stenseng, A. Zolin, R. Cenni, F. Frandsen, A. Jensen and K. Dam-Johansen, J. Therm. Anal. Cal., 64 (2001) 1325.
17 X. H. Liang and J. A. Kozinski, Fuel, 79 (2000) 1477.
18 L. A. Hansen, F. J. Frandsen, K. Dam-Johansen and S. Sorensen, Thermochim. Acta, 326 (1999) 105.
19 S. K. Gupta, T. F. Wall, R. A. Crelman and R. P. Gupta, Fuel Process. Technol., 56 (1998) 33.
20 S. Arvelakis, C. Sotiriou, A. Moutsatsou and E. G. Koukios, J. Therm. Anal. Cal., 56 (1999) 1271.
21 S. Arvelakis and F. J. Frandsen, Fuel, 84 (2005) 1725.
22 S. Arvelakis, P.-A. Jensen and K. Dam-Johansen, Energy Fuels, 18 (2004) 1066.
23 CRC Handbook of Chemistry and Physics, 77th Ed., 1996–1997.

DOI: 10.1007/s10973-006-8221-y